

Muon detection studied by pulse-height energy analysis: Novel converter arrangements

Cite as: Rev. Sci. Instrum. **86**, 083306 (2015); <https://doi.org/10.1063/1.4928109>

Submitted: 03 June 2015 . Accepted: 25 July 2015 . Published Online: 06 August 2015

Leif Holmlid , and Sveinn Olafsson



View Online



Export Citation



CrossMark

ARTICLES YOU MAY BE INTERESTED IN

[Heat generation above break-even from laser-induced fusion in ultra-dense deuterium](#)

AIP Advances **5**, 087129 (2015); <https://doi.org/10.1063/1.4928572>

[Production of ultradense deuterium: A compact future fusion fuel](#)

Applied Physics Letters **96**, 124103 (2010); <https://doi.org/10.1063/1.3371718>

[Phase transition temperatures of 405-725 K in superfluid ultra-dense hydrogen clusters on metal surfaces](#)

AIP Advances **6**, 045111 (2016); <https://doi.org/10.1063/1.4947276>



MCL
MAD CITY LABS INC.

AFM & NSOM Nanopositioning Systems Micropositioning Single Molecule Microscopes



Muon detection studied by pulse-height energy analysis: Novel converter arrangements

Leif Holmlid^{1,a)} and Sveinn Olafsson²

¹*Atmospheric Science, Department of Chemistry and Molecular Biology, University of Gothenburg, SE-412 96 Göteborg, Sweden*

²*Faculty of Physical Sciences, University of Iceland, Reykjavik, Iceland*

(Received 3 June 2015; accepted 25 July 2015; published online 6 August 2015)

Muons are conventionally measured by a plastic scintillator–photomultiplier detector. Muons from processes in ultra-dense hydrogen H(0) are detected here by a novel type of converter in front of a photomultiplier. The muon detection yield can be increased relative to that observed with a plastic scintillator by at least a factor of 100, using a converter of metal, semiconductor (Ge), or glass for interaction with the muons penetrating through the metal housing of the detector. This detection process is due to transient formation of excited nuclei by the well-known process of muon capture, giving beta decay. The main experimental results shown here are in the form of beta electron energy spectra detected directly by the photomultiplier. Events which give a high-energy tail in the energy spectra are probably due to gamma photons from the muons. Sharp and intense x-ray peaks from a muonic aluminium converter or housing material are observed. The detection conversion in glass and Ge converters has a time constant of the order of many minutes to reach the final conversion level, while the process in metal converters is stabilized faster. The time constants are not due to lifetimes of the excited nuclei or neutrons but are due to internal charging in the insulating converter material. Interaction of this charging with the high voltage in the photomultiplier is observed. © 2015 AIP Publishing LLC. [<http://dx.doi.org/10.1063/1.4928109>]

I. INTRODUCTION

Both positive and negative muons are formed naturally in the upper atmosphere¹ from impact of particles with cosmic origin. They move down to the surface of Earth and into the ground despite their short lifetime.^{1,2} Muons are the final unstable particles formed by meson decay³ and decay themselves (at 2.2 μ s, thus, slower than any mesons) to electrons or positrons plus neutrinos. Muons can be produced at large flux densities by high-energy (hundreds of GeV) protons impacting targets at so called muon factories, for example, at CERN-SPS (Super Proton Synchrotron).⁴ The research on muons is also coupled to the production of neutrinos at so called neutrino factories.⁵ Here, muons formed by nuclear processes in ultra-dense hydrogen H(0)^{6,7} are studied by their interaction with solid converter materials. These interactions give both electrons and x-ray photons which are detectable by photomultipliers (PMTs). The electrons and x-ray photons are here studied by pulse-height energy analysis giving characteristic energy spectra. The practical instrumental goal is to measure the intensity and energy of muons with a small device, to be able to assess the risks of small-scale fusion devices which may emit large fluxes of muons.⁸

Ultra-dense hydrogen has been studied mainly in our group for several years.⁶ It is normally indicated as H(0) and has been studied in the two forms of ultra-dense deuterium D(0)⁹ and ultra-dense protium p(0).¹⁰ Due to the extremely high density of this material with interatomic distances normally of 2.3 pm,⁷ it is expected that it will be an excellent

fuel for laser-induced nuclear fusion.^{11–13} The density of this fuel is so high that further compression is not needed to reach fusion conditions, but only an igniting laser pulse. Laser-induced fusion processes have, indeed, been reported.^{9,11,12} Such fusion processes have been observed by mass spectrometry to give both ³He and ⁴He.¹⁴ The fast particles at >10 MeV u⁻¹ observed from the laser-induced processes in H(0) also indicate nuclear processes.^{12,15–17} The particle energy is high enough to give electron-positron pair production.¹⁸ These MeV u⁻¹ particles decay in a few ns to other particles.¹⁹ The lifetimes of the MeV u⁻¹ particles agree with those for kaons and pions³ which all decay forming muons. In our thermal (calorimetric) laser-induced fusion experiments in D(0) (in press), a substantial fraction of the total particle energy from the fusion process was not measurable. It was leaking out in an unidentified way, apparently as penetrating particles but not as neutrons. A search was then initiated to identify gamma radiation or other high-energy particles. This resulted in detection of very intense beta-like energy spectra and line spectra due to muons. It appears likely that many small-scale fusion test systems emit muons, and it is thus important to understand how to selectively detect muons with high sensitivity. Progress in this direction is now reported.

Muons are often observed by detectors composed of a plastic scintillator (PS) and a PMT.^{20,38} The muon signal is here detected with much higher signal yield after converting the muons more effectively into electrons with energy distributions similar to beta distributions. This conversion method for muon detection has not been reported previously. The beta electrons are observed directly by the PMT. The detection mechanism responds to muons entering the detector through a thick metal enclosure. The muons fall with a large probability

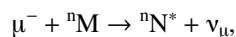
^{a)}Email: holmlid@chem.gu.se

into low-energy levels around the nuclei in the materials close to the PMT cathode, forming muonic atoms.²¹ The subsequent capture into the nucleus normally transfers a proton in the nucleus to a neutron, giving an excited nucleus with atomic number decreased one step. This excited nucleus decays relatively rapidly by beta decay. In reality, the processes are more complex varying also with the energy of the captured muons, so other nuclei and other particles than electrons may also be formed by the nuclear decay. The general principles of the muon capture are well known,² but for each different nucleus, several different outcomes are possible.

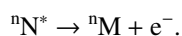
II. THEORETICAL BACKGROUND

Ultra-dense hydrogen H(0) is a quantum material at room temperature. It is described in several publications, with detailed studies of the structure of the two isotope forms D(0)^{7,22} and the protium analog p(0).²³ H(0) is a spin-based Rydberg matter⁷ with angular momentum $l = 0$ for the electrons. It is shown to be both superfluid²⁴ and superconductive (Meissner effect observed) at room temperature.²⁵ H(0) may involve formation of vortices in a Cooper pair electron fluid as suggested by Winterberg.^{26,27} Due to the measured very short H–H distances of 2.3 pm,^{22,28} the density of H(0) is very high, in fact higher than the density of hydrogen fuel for fusion believed possible by any compression method. Thus, it should be possible to initiate nuclear fusion by relatively weak laser pulses in the ultra-dense deuterium D(0) material.^{9,11,12} It is likely that the main process initiated by the laser pulse is a transition from level $s = 2$ with D–D distance of 2.3 pm to level $s = 1$ with distance 0.56 pm^{7,13} from where fusion is spontaneous. If this transition to level $s = 1$ can take place spontaneously, a spontaneous fusion process is possible similar to the ones named LENR (Low Energy Nuclear Reactions).^{29,30} Several studies have proved the formation of MeV particles from D(0) during laser impact under conditions useful for ICF (Inertial Confinement Fusion).^{9,11,12,15–17} Particle energies up to 20 MeV u^{-1} have been observed.^{15,17} Recent studies (submitted) show that most high-MeV particles are neutral, probably cluster fragments $H_N(0)$ of ultra-dense matter H(0)²³ with a typical size of only a few pm. They seem to convert rapidly to several types of mesons.¹⁹

Muons interact with matter by first forming a muonic atom, with the muon in a low orbit close to the nucleus. This process gives gamma radiation, for example, similar to K α radiation.²¹ The muon is then often captured into the nucleus, giving an excited nucleus with a proton replaced by a neutron as, for example,²

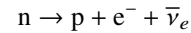


where atomic number $Z_N = Z_M - 1$ and n is the mass number. This may be followed by many different processes of which beta decay is most interesting here due to the measured energy distributions,

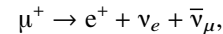
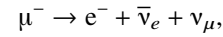


The energy of the emitted electron will vary with the isotopes formed and the excess energy in the excited nucleus. Another common process from the excited nucleus is neutron ejection.²

The kinetic energy of the neutrons will often be relatively low, peaking towards low energy of a few MeV.² The neutrons will decay with a lifetime of 15 min as



giving electrons with maximum energy $Q = 782$ keV.³¹ The decay of free muons with lifetime 2.2 μs is also possible as part of the signal detected. This takes place as



but the electrons and positrons formed do not have the typical beta-like energy distribution but peak at higher energy closer to Q .²

III. EXPERIMENTAL

Two different sources for producing H(0) have been used for this study. They are similar to a source described in a previous publication.²⁸ Potassium-doped iron oxide catalyst samples (cylindric pellets)^{32,33} in the sources produce the ultra-dense H(0) from hydrogen or deuterium gas flow at pressures of 10^{-5} –100 mbars. The sources give a slowly decaying muon signal for several hours and days after being used for producing H(0). They can be triggered to increase the muon production by laser irradiation inside the chambers or sometimes even by turning on the fluorescent lamps in the laboratory for a short time.

The PMT detector part is used in several different forms. Its light-tight enclosure is built from high-vacuum metal KF (klein-flansch) components of 40 mm inner diameter. The components inside the housing are scintillators, converters of metal, glass or other materials, metal foils, and a PMT. The PS is of type BC408 (Saint-Gobin)³⁷ and has 40 mm diameter and length 50 mm. The PS gives mainly blue photons (maximum emission at 423 nm). The metal converters are plates, discs, lumps, or pieces of metals like Cu, Mn, steel, Pb, Al, or Au. The glass converter with diameter 25 mm and thickness 3 mm is normally a metal-ion containing blue-green glass filter (Schott BG3, 3 mm thick) but also other types from Schott are used. Also, clear glass filters (thickness up to 6 mm) and milky glass filters have been used. The semiconductor converter used is a germanium (Ge) window (Janos Technology) with thickness 2 mm and diameter 25 mm. An Al foil of thickness 20 μm is sometimes used, cut to 25 mm diameter. The PMT used is Electron Tubes 9128B with single electron rise time of 2.5 ns, electron transit time 30 ns, end-window cathode, and linear focused dynode structure. The cathode is at negative high voltage (HV) of 1600 V. Its diameter is 29 mm. The converters are mounted on the PMT window with black plastic tape winding. The final detector part is shown in the photo in Fig. 1. A preamplifier (Ortec VT120) with bandwidth 10–350 MHz and gain 200 and a pulse-shaping amplifier (Ortec 440A) with shaping time 0.5 μs were normally used. Also, other amplifiers like Ortec VT120 with nominal gain 20 and pulse-shaping amplifier Ortec 575A were employed. The signal from the PMT was analyzed by a 2048 channel multi-channel analyzer (MCA) (Ortec EASY-MCA-2k with Maestro software) for the

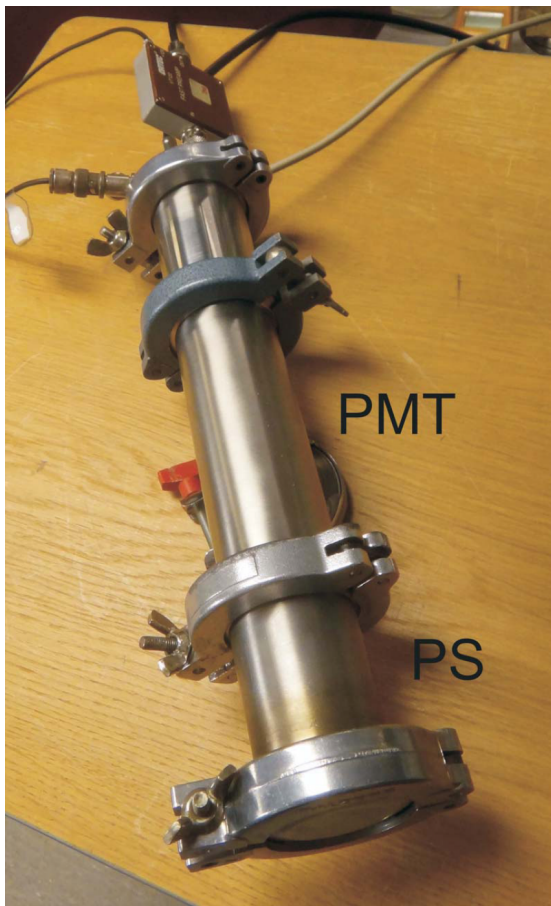


FIG. 1. Detector part from vacuum components. The PMT part and the PS part are indicated. Without the PS part, a metal blind flange is used to close the tube.

MCA spectra of 500 s duration. When the converter is to be changed, the PMT enclosure is opened and closed in darkness, with the HV off, with no other change in position of the detector. Another MCA was also used, giving the same beta-like distributions. Most experiments were run in darkness, even with black cloth covering the detector parts to avoid any light leakage.

The electron energy scale of the PS is calibrated by measuring the beta emission from a ^{137}Cs probe (37 kBq, Gammadata, Uppsala, Sweden). Measurements are made in air with and without a 20 μm thick Al foil in front of the scintillator. The shifting of the beta signal with a blue-filter in front of the PMT is verified, proving that the beta particles interact with the PS. A plot of the square root of the number of counts (signal-background) (Kurie-like plot) gives zero signal due to ^{137}Cs at 765 channels with gain = 1 in the amplifier Ortec 440 A and gain 200 in the preamplifier. $Q = 512$ keV gives the approximate calibration of 0.67 keV/channel. A similar calibration of only the PMT in Fig. 2 without the PS gives zero intercept signal due to ^{137}Cs at 170 channels with the same electronics. This gives an approximate calibration of 3.0 keV/channel. A tentative linear scale is used to tag the various features relative to these calibrations.

The time variation of the total signal was measured by a multi-channel scaler (MCS) with 1 s dwell time per channel (EG&G Ortec Turbo-MCS). The pulse signal from the

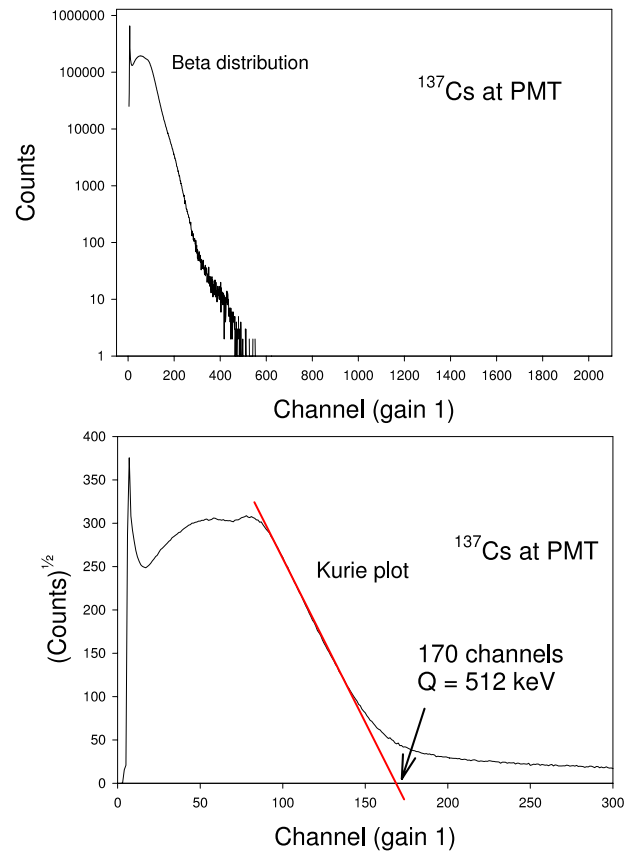


FIG. 2. A ^{137}Cs probe at the PMT with no metal flange. The approximate Kurie plot shows the zero signal intercept at 170 channels corresponding to $Q = 512$ keV.

PMT was analyzed after recording by a fast digital oscilloscope (Tektronix TDS 3032, 300 MHz). A GM detector (Rados RDS-80) gives slightly higher signal where the PMT indicates enhanced external signal. The gamma signal was measured with Mirion Technologies PDS-100G without any higher signal detected at the apparatus. In Table I, some ranges of interest for electrons and muons in Fe, Al, and in the scintillator material are collected.

The place of origin of the beta-type signal must also be known. From tests with a ^{137}Cs beta emitter, it is apparent that beta electrons even with relatively high energy ($Q = 512$ keV) cannot penetrate the thick metal walls used here for the PMT enclosure without large energy loss. Thus, the electrons

TABLE I. Ranges for a few energies of electrons and negative muons in the materials used. Data from the electron database at NIST,³⁶ from muon ranges in Ref. 39 and from manufacturer's data.³⁷

| Particle | Energy (MeV) | Range in steel (mm) | Range in Al | Range in plastic scintillator (μm) | Range in air (m) |
|----------|--------------|---------------------|-------------------|---|------------------|
| e^- | 0.03 | | 9 μm | 10 | 0.018 |
| e^- | 0.1 | | 69 μm | 150 | 0.143 |
| e^- | 0.3 | | 410 μm | 700 | 1.1 |
| e^- | 1 | 0.77 | 2.0 mm | 4000 | 4.4 |
| e^- | 10 | 7.6 | 26 mm | | 46 |
| μ^- | 10 | 1.3 | 3.4 mm | | 7.1 |
| μ^- | 20 | 4.3 | 11.4 mm | | 24 |

observed in the low-energy beta-like distributions in the muon experiments are definitely formed inside the PMT enclosure by penetrating particles. These low-energy distributions observed in the experiments are typical for beta-decay. They have the correct type of energy spectrum and give linear Kurie-like plots.³¹ They do not agree with the electron energy distributions from muon decay.² The same shape giving linear Kurie-like plots is found by using a beta emitter ^{137}Cs without a scintillator, thus with the beta electrons with $Q = 512$ keV penetrating into the PMT. (The same shape is also found with a PS, but with higher pulse energies giving another calibration as described above.) These results are used to calibrate the beta energy scale. This means that the beta-like distribution is due to electrons from beta decay of either unstable nuclei or free neutrons in the converter.

IV. RESULTS

A. Muon signal

The PS was combined with only a PMT for standard muon measurements in the present experiments. Such a detector gives a signal consisting of a low-energy beta-type distribution similar to those from the other converters, and a high-energy tail which is caused by pulses of several blue photons from the PS (emission maximum at 423 nm). This property of the tail is demonstrated by inserting a grey filter with OD2 (1% transmission) between the PS and the PMT, which removes the tail as shown in Fig. 3 since the photons are absorbed by the filter. This signal from the PS is normally used for muon detection. Note that the beta distribution does not change with the grey filter; thus, it is not due to visible photons. A blue-filter shifts the tail towards lower energies, since the number of photons in each multi-photon pulse is decreased by the filter. Thus, the tail is due to high-energy particles like muons entering the PS through the 2 mm thick steel enclosure. The beta distribution intensity is increased more than a factor of 10 by the blue-filter.

In experiments using the PS, a crude division of the energy spectrum into the low-energy beta distribution and the

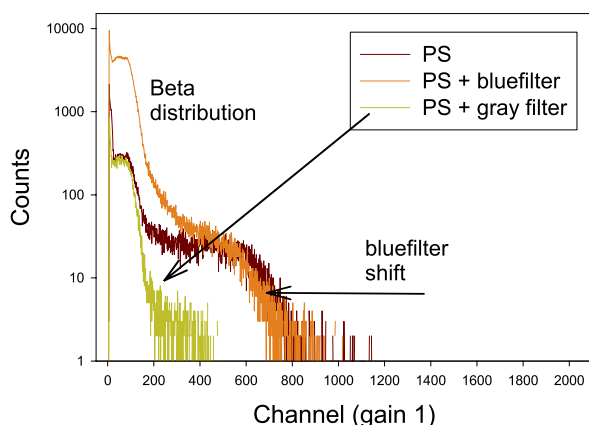


FIG. 3. Demonstration of visible light photons from the PS to the PMT in the tail of the distribution due to particle interaction with the PS, and of penetrating particles to the PMT in the low-energy distribution. Conversion by the colored glass filter is clearly observed.

high-energy tail was made. The low-energy count (which is much larger than the tail) varied from 1.3×10^5 at start on one day with cold source in one apparatus to $2.6\text{--}3.2 \times 10^5$ with the source in operation. With the standard deviation σ of 360-566 of these numbers according to Poisson statistics, the increase is 260 times larger than σ and thus statistically ascertained. With the source turned off at the end of the experiments, the count was 1.6×10^5 thus a certain change due to the source. In another experiment, the count was 1.08×10^5 at another source, sinking to 0.91×10^5 2 m away. The standard deviation is around 300 while the difference is 17 000, thus >50 times larger. Thus, a clear shift with detector position is found. The high-energy tail in these experiments (which is due to the particles giving photons in the PS, not electrons in the beta distribution) was close to 7000, thus with a standard deviation $\sigma = 80$. With water and lead shielding, the count was 7300 while without the shielding, the count was >8300 , thus a difference 12 times larger than σ . A position close to one source which was not operating gave a count of 6915, while directly moving the detector a 3 m long distance from that position gave a count of 7873, thus a change 12 times larger than σ . A higher signal far from the source indicates a decay of the emitted particles. It is concluded that a signal due to decaying particles and muons exists in the laboratory.

B. Metal converters

The most interesting results from a detection point of view are found with converters of metal. In Fig. 4, the behavior

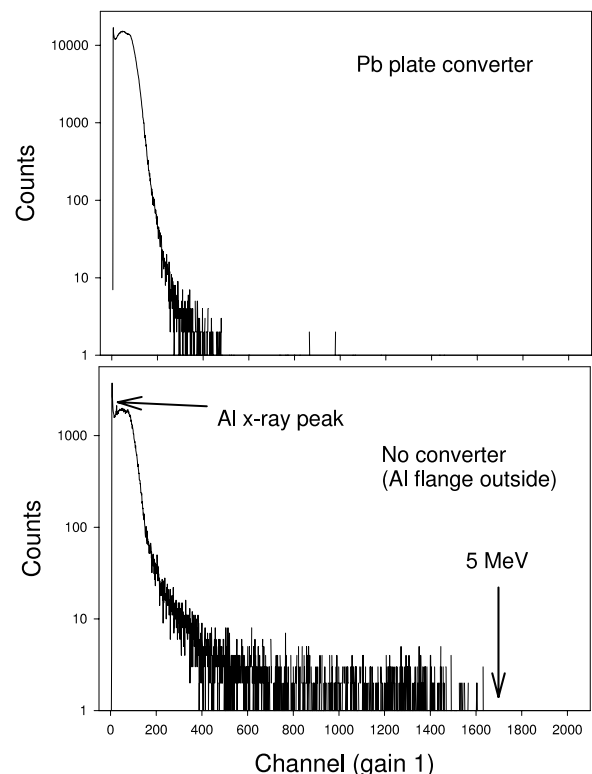


FIG. 4. A Pb metal converter with relatively low conversion relative to the case with no converter shown in the lower panel. The Pb plate (with no opening) converter removes both the high-energy tail and the x-ray peak due to the outer Al flange.

of Pb is compared to that without converter with a similar high particle production in the source 1 h later. In both cases, a flange of 3 mm thick Al encloses the cathode end of the detector part in which the PMT is contained. The signal with the 2 mm thick Pb plate increases the signal around a factor of five at low energy, with a broad maximum around 150 keV. The high-energy tail at up to 5 MeV energy without a converter (thus from the Al flange) is not observed with the Pb converter. This kind of difference for different parts of the spectrum gives further information, in this case, that the tail is probably due to photons which are not transmitted by the Pb plate. Thus, they may be soft x-ray photons. With other metals like Al and Cu, both a large low-energy signal and a large high-energy tail are found as shown in Fig. 5. Other metals like Mn do not give a high-energy tail at all and a low maximum signal. These details are certainly related to the properties of the excited nuclei formed for each metal but the explanation is probably quite complex.

Kurie-like plots invariably show a linear behavior, as in Fig. 5. The zero-signal cutoff normally falls between 150 and 200 channels at gain = 1 with some systematic variation for different metals. This means a Q value for the beta processes of 450-600 keV according to the calibration of the PMT.

In many experiments, a sharp peak is observed in the energy spectra as in Fig. 6, close to 75 keV from the PMT beta calibration. Its origin is here Al, either from an Al converter or from the Al flange used in the PMT enclosure. Electrons are not likely to give such a sharp peak, but its skewed shape suggests that scattering losses exist. It is probably due to x-ray

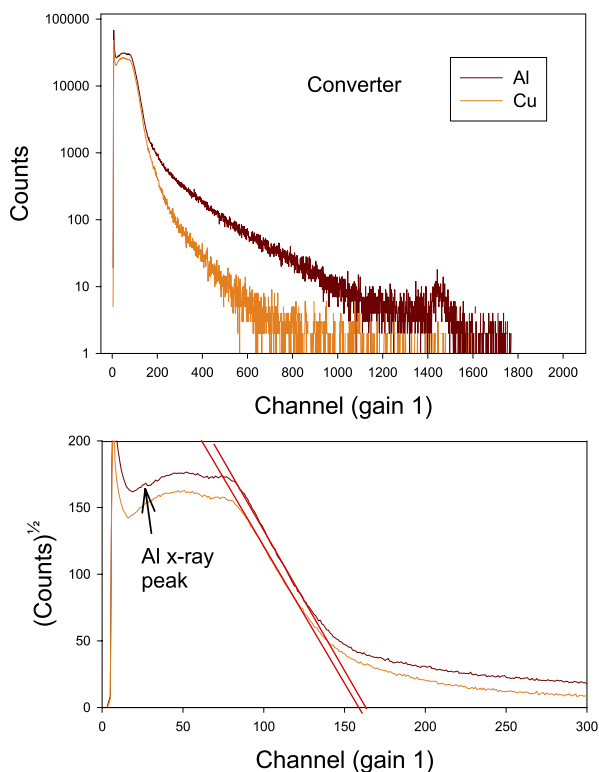


FIG. 5. Typical energy spectra using the best tested converter metals Al and Cu. The high-energy tail is very pronounced, even showing a maximum at 1450 channels or 4.35 MeV for the Al converter. The Kurie-like plots in the lower panel show a linear behavior.

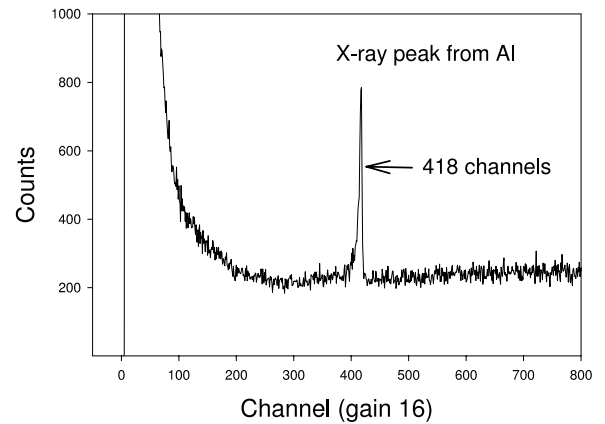


FIG. 6. X-ray peak due to Al in the outer flange, of this large size for just a few minutes. This line is suggested to be the muonic Al atom transition $2p-1s$ which is at 346.8 keV.³⁴

photons from the formation of the muonic Al atom. The line shape for such processes is very similar to the one found here.²¹ The most prominent line for Al is the $2p-1s$, at 347 keV.³⁴ This may give a calibration of other x-ray signals entering the PMT. Small peaks of a similar type are sometimes detected.

C. Semiconductor converter

The only semiconductor converter tested is Ge. It gives a relatively high and constant amplification. The insertion of a non-metal converter gives an increase in the signal level which has a time constant up to 2 h (Fig. 7). Often there is no change at all for a considerable time (to the left in the figure) after which a rapid switch in the signal generation takes place. Normally, the low-energy distribution increases first, with the high-energy tail increasing rapidly somewhat later. If the converter is removed, the fall of the signal to typical background level is immediate. Also an interaction with the HV exists, such that a time delay from low to high signal exists after the HV for the PMT is connected. It is also possible to observe a signal fall with a similar time constant by using two converters and removing one of them.

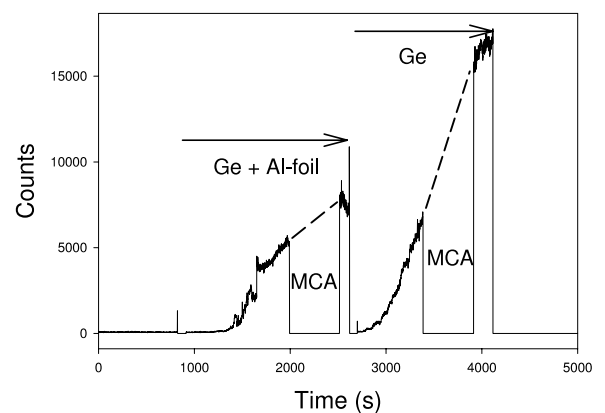


FIG. 7. Time variation of the total pulse signal in counts/s from the PMT using Ge as converter with the MCS. The first part also includes an Al foil between the Ge and the PMT, giving a lower signal. Time constants are a few minutes. During the periods marked MCA, the signal was redirected to the MCA.

D. Insulator converters

Many different types of glass filters have been tested for the muon detection. Insulators show time constants in the detection in the same way as semiconductors. The time variation of the signal has been studied and the relevant time constants have been found. For glass converters, they are in the range 5-140 min and vary mainly with the thickness of the glass. This indicates that the time delay is due to an interaction between the HV and the charges set free by the external particle radiation in the insulating material. How this effect can influence the electrons released in the converter is not fully understood.

E. Enclosure

The metal enclosure of the converter and PMT detector has a direct influence on the signal observed. In Fig. 8, four consecutive experiments are shown of the low-energy distribution (gain = 16). Without an Al flange at the converter-cathode end of the enclosure (here, in darkness and with several layers of black cloth coverage), the signal is much lower, down a factor of 10-50. (That the cloth would give such a strong signal reduction is unlikely due to its low mass relative to the metal flange.) Also, the shape of the low-energy distribution is different, with a Kurie-like linear part having zero signal cutoff at 300/16 channels thus at approximately $Q = 56$ keV. The influence of the Al converter is directly seen in Fig. 8. Note that the Al flange runs were done before and after the other runs to control that the muon source intensity did not change significantly.

V. DISCUSSION

A. Expected particles

The mechanism giving the particles from the sources used is not fully understood but involves nuclear processes in the

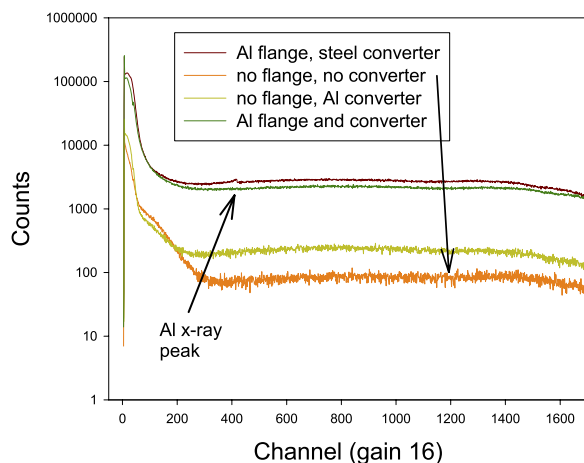


FIG. 8. Combined influence of the converter and of the flange capping the detector part. No flange means that thick black cloth is used to stop any light (in darkness) from reaching the PMT cathode. The same cloth with a flange in place did not change the signal appreciably. The Al gamma peak is not always visible, which may indicate the presence of other exciting particles than negative muons.

ultra-dense hydrogen $H(0)$. Since it seems that kaons and pions are formed from $H(0)$,³⁵ both positive and negative muons should exist in the particle flux to the detector, being formed by decay from these mesons. Only negative muons can give muonic atoms and muon capture, and thus the two main features observed, the beta distributions and the sharp x-ray peaks are due to negative muons. It may be considered that the high-energy tail in the spectra from the converters is due to positive muons, but no clear evidence exists. However, since a large low-energy signal and a high-energy tail often appear suddenly and almost simultaneously in experiments with glass converters, the particle flux under such conditions may be charge compensated and contain both negative and positive muons at similar flux densities, thus removing the charge barriers that seem to exist in the glass converters. This would then give the apparent low-energy and the high-energy parts of the spectra from these two particle fluxes of negative and positive muons.

B. Energy distributions

In the Kurie-like plots, the zero signal cutoff (intercept) is close to 170 channels or 510 keV according to the energy calibration of the PMT. The actual value varies with the combination of converter materials used. However, the zero-signal cutoff does not vary with the momentary conversion gain in the converter. That this value is the same independent of the size of the actual signal means that it is of fundamental origin.

Even if the shape of the Kurie-plot is constant independent of many parameters like the intensity of the muon signal, this is not the case for the shape of the maximum of the low-energy distribution, at energies lower than the Kurie-slope. It often becomes more flat at low conversion yield and with a clear maximum at high conversion. The energy distribution at high conversion normally also displays a long high-energy tail, up to energies corresponding to at least 5 MeV. It often displays a maximum at high energy as in Fig. 5. The high-energy tail is not transient but can exist almost unchanged during a whole day of experiments.

The intrinsic background in the PMT does not have an extended Kurie-like shape and does not give a well-defined constant zero signal cutoff. The intrinsic background neither has a high-energy tail. This means that the signal of interest here is characterized both by the Kurie-like plots and by the high-energy tail observed at high conversion gains.

C. Time constants

It might be tempting to identify the time constants of the signal, for example, in Fig. 7 as due to neutron decay giving the beta-type energy distributions with $Q = 782$ keV. The decay time of free neutrons is around 15 min or 900 s, and the observed time constants in Fig. 7 are close to this value. The calibration of the PMT response with ^{137}Cs gives approximately 3 keV per channel at gain = 1. This would give a Q of 260 channels in the spectra, which is considerably higher than any observed value of Q . It is possible that the

energy scale in the PMT is not linear. If that is the case, neutron decay may be part of the signal observed using semiconductors and insulators as converters.

Tests with glass converters tend to give longer time constants for thicker glass. Thus, the time constants are more likely due to charging effects in the insulating materials. The signals are not smooth in time but vary with spikes and other features that indicate charging and discharging phenomena in the materials. Also, the influence of the high voltage of the PMT indicates that this is a plausible explanation.

D. Muon intensity

The muons may of course have high enough energy to pass through the converters used. This implies that not all muons are detected even at the highest measured signal levels. However, the total detected signal can be calculated from the number of total counts in each run, or from the number of pulses per second, for example, at the high counting rate of 15 kilocounts/s in Fig. 7. The converter was in this case a 3 mm thick glass filter with diameter 25 mm. At 2 m from the source, the total angular coverage of the converter was 10^{-5} sr. This means a total intensity of 1.5×10^9 s⁻¹ sr⁻¹. Assuming this value to be slightly too high due to multiple peaks from single events in the high-energy tail is realistic. Thus, a reasonable (conservative) value is approximately 10^9 s⁻¹ sr⁻¹. If each such initial particle carries the energy observed by the MeV TOF studies^{17,18} of 20 MeV u⁻¹, the total energy ejected as kinetic energy of the muons is 3 mW sr⁻¹. If this is due to spontaneous fusion of D(0) to ⁴He in the source, each pair of 20 MeV u⁻¹ particles requires the fusion of approximately 6 D atoms (giving 43 MeV). This means a total number of D atoms required for this energy release of 6×10^9 s⁻¹ sr⁻¹ or 1×10^{-14} mol s⁻¹ sr⁻¹. During one year, this means a fusion consumption of close to 7 μg of deuterium. If the initial ejected particles are lighter than one mass unit u, the final numbers are reduced in proportion. In this discussion, it is excluded that the muons are formed from the fusion energy, but it is clear that they are formed from nuclear and decay processes starting in the D(0). So the total number of D atoms lost from the system has to be increased by approximately 1/6 or 17%. These numbers appear quite realistic and the muon generation does not imply a large energy release which might be observed by other methods.

E. Particle penetration

In Table I, a few values of the tabulated ranges of the different particles are collected. Muons with >20 MeV energy will move many meters in air as seen in the table. They move >400 m during their lifetime of 2.2 μs. They also penetrate into the detector housing with its wall of a few mm steel or Al. On the other hand, they probably do not pass through the PS at several cm length if they do not have more than 20 MeV energy. So the low-energy signal observed with the PS is probably caused by muons which move directly into the converter through the steel wall. Electrons from beta processes outside the detector housing with energies of below 1 MeV will not penetrate without energy loss into the housing, as concluded

above from direct measurements. They will however move into the PMT from the converter, as also seen directly in the experiments. Such electrons should also be able to pass through the air from the wall of the detector housing, even if the wall (flange) is at several cm distance from the PMT and converter. That a large signal is not observed by such arrangements is probably due to loss in intensity of the randomly directed electron flux by the increased distance between the end flange and the PMT.

VI. CONCLUSIONS

More efficient detection of muons is shown to be possible by the use of solid converters utilizing muon capture, combined with a photomultiplier. Since muons appear to be formed in small-scale nuclear fusion devices, it is important to find methods to measure muon fluxes efficiently. Muons may also become useful for atomic analysis by the x-rays emitted during the formation of muonic atoms.

ACKNOWLEDGMENTS

The construction of part of the apparatus used was supported by GU Holding, The Holding Company at University of Gothenburg.

- ¹M. F. L'Annunziata, in *Handbook of Radioactivity Analysis* (Elsevier, 2012), chap. 1.
- ²D. F. Measday, *Phys. Rep.* **354**, 243 (2001).
- ³W. E. Burcham and M. Jobes, *Nuclear and Particle Physics* (Pearson Education, Harlow, 1995).
- ⁴R. Webb on behalf of the COMPASS collaboration, *Nucl. Phys. A* **755**, 329c (2005).
- ⁵M. M. Alsharo'a, C. M. Ankenbrandt, M. Atac, B. R. Autin, V. I. Balbekov *et al.*, *Phys. Rev. Spec. Top.: Accel. Beams* **6**, 081001 (2003).
- ⁶S. Badiéi, P. U. Andersson, and L. Holmlid, *Int. J. Hydrogen Energy* **34**, 487 (2009).
- ⁷L. Holmlid, *Int. J. Mass Spectrom.* **352**, 1 (2013).
- ⁸L. Holmlid and S. Olafsson, *Int. J. Hydrogen Energy* **40**, 10559 (2015).
- ⁹S. Badiéi, P. U. Andersson, and L. Holmlid, *Laser Part. Beams* **28**, 313 (2010).
- ¹⁰F. Olofson and L. Holmlid, *Nucl. Instrum. Methods B* **278**, 34–41 (2012).
- ¹¹P. U. Andersson and L. Holmlid, *J. Fusion Energy* **31**, 249 (2012).
- ¹²L. Holmlid, *Nucl. Instrum. Methods B* **296**, 66 (2013).
- ¹³L. Holmlid, *J. Fusion Energy* **33**, 348–350 (2014).
- ¹⁴F. Olofson and L. Holmlid, *Int. J. Mass Spectrom.* **374**, 33 (2014).
- ¹⁵L. Holmlid, *Laser Part. Beams* **31**, 715 (2013).
- ¹⁶L. Holmlid, *Eur. Phys. J. A* **48**, 11 (2012).
- ¹⁷L. Holmlid, *Int. J. Modern Phys. E* **22**, 1350089 (2013).
- ¹⁸F. Olofson and L. Holmlid, *Laser Part. Beams* **32**, 537 (2014).
- ¹⁹L. Holmlid, *Int. J. Modern Phys. E* **24**, 1550026 (2015).
- ²⁰M. F. L'Annunziata, *Handbook of Radioactivity Analysis*, 2nd ed. (Elsevier, USA, 2003).
- ²¹H. J. Evans, *Nucl. Phys. A* **207**, 379 (1973).
- ²²L. Holmlid, *J. Cluster Sci.* **23**, 5 (2012).
- ²³L. Holmlid, *Int. J. Mass Spectrom.* **351**, 61 (2013).
- ²⁴P. U. Andersson and L. Holmlid, *Phys. Lett. A* **375**, 1344 (2011).
- ²⁵P. U. Andersson, L. Holmlid, and S. R. Fuelling, *J. Supercond. Novel Magn.* **25**, 873 (2012).
- ²⁶F. Winterberg, *J. Fusion Energy* **29**, 317 (2010).
- ²⁷F. Winterberg, *Phys. Lett. A* **374**, 2766 (2010).
- ²⁸P. U. Andersson, B. Lönn, and L. Holmlid, *Rev. Sci. Instrum.* **82**, 013503 (2011).
- ²⁹E. Storms, *The Science of Low Energy Nuclear Reaction* (World Scientific Publishing Company, 2007).
- ³⁰E. Storms, *The Explanation of Low Energy Nuclear Reaction* (Infinite Energy Press, 2014).

- ³¹K. S. Krane, *Introductory Nuclear Physics* (Wiley, Hoboken, 1988).
- ³²G. R. Meima and P. G. Menon, *Appl. Catal. A* **212**, 239 (2001).
- ³³M. Muhler, R. Schlögl, and G. Ertl, *J. Catal.* **138**, 413 (1992).
- ³⁴D. F. Measday, T. J. Stocki, B. A. Mofteh, and H. Tam, *Phys. Rev. C* **76**, 035504 (2007).
- ³⁵L. Holmlid, "Decay of charged nuclear particles at 13 and 26 ns formed by laser-induced processes in ultra-dense hydrogen," *Ann. Phys.* (submitted).
- ³⁶National Institute of Standards and Technology NIST, Physics Laboratory, ESTAR Program, 2015.
- ³⁷Saint-Gobain Products, *Scintillation Products Organic Scintillation Materials*, 2001-11.
- ³⁸W. R. Leo, *Techniques for Nuclear and Particle Physics Experiments*, 2nd ed. (Springer, Berlin Heidelberg, 1994).
- ³⁹D. E. Groom, N. V. Mokhov, and S. I. Striganov, *At. Data Nucl. Data Tables* **78**, 183 (2001).